Inorg. Chem. **2007**, *46*, 11345–11355

Structural Comparisons of Silver(I) Complexes of Third-Generation Ligands Built from Tridentate (o-$C_6H_4[CH_2OCH_2C(pz)_3]_2$) versus Bidentate Poly(1-pyrazolyl)methane Units (o-$C_6H_4[CH_2OCH_2CH(pz)_2]_2$) (pz = Pyrazolyl Ring)

Daniel L. Reger,* Elizabeth A. Foley, Radu F. Semeniuc, and Mark D. Smith

Department of Chemistry and Biochemistry, University of South Carolina, Columbia, South Carolina 29208

Received September 10, 2007

The new bitopic, bis(1-pyrazolyl)methane-based ligand o-$C_6H_4[CH_2OCH_2CH(pz)_2]_2$ (**L²**, pz = pyrazolyl ring) is prepared from the reaction of $(pz)_2CHCH_2OH$ (obtained from the reduction of $(pz)_2CHCOOH$ with $BH_3{\cdot}S(CH_3)_2$) with NaH, followed by the addition of α,α′-dibromo-o-xylene. The reaction of **L²** with $AgPF_6$ or AgO_3SCF_3 yields $\{o\text{-}C_6H_4[CH_2OCH_2CH(pz)_2]_2(AgPF_6)\}_n$ or $\{o\text{-}C_6H_4[CH_2OCH_2CH(pz)_2]_2(AgO_3SCF_3)\}_n$, respectively. Both compounds in the solid state have tetrahedral silver(I) centers arranged in a 1D coordination polymer network. The analogous ligand based on tris(1-pyrazolyl)methane units, o-$C_6H_4[CH_2OCH_2C(pz)_3]_2$ (**L³**), reacts with AgO_3SCF_3 to form a similar coordination polymer, $\{o\text{-}C_6H_4[CH_2OCH_2C(pz)_3]_2(AgO_3SCF_3)\}_n$. In this case, each tris(pyrazolyl)methane unit in **L³** adopts the κ^2–κ^0 bonding mode. Crystallization of a 3:1 mixture of AgO_3SCF_3 and **L³** yields $\{o\text{-}C_6H_4[CH_2OCH_2C(pz)_3]_2(AgO_3SCF_3)_2\}_n$, in which the tris(1-pyrazolyl)methane units adopt a κ^2–κ^1 coordination mode.

Introduction

Significant efforts directed toward the design of specific architectures formed by the self-assembly processes have been carried out in a number of fields of synthetic chemistry.[1] The synthesis and characterization of coordination polymers with designed structures and properties has been one important area.[2] In this work, the features that control the structures of coordination polymers are the ligand topicity, flexibility or rigidity of the linker groups joining the coordination sites, and the stereochemical preferences of the coordinated metal ion.[1b−f,3] Also important is the role of noncovalent interactions that add further organization into more complex networks. Many interactions involving the anions[3a−d,4] and the solvents[2g,3b,5] were found to have an impact on the crystal packing of a variety of compounds. The most important forces impacting the supramolecular

* To whom correspondence should be addressed. E-mail: reger@mail.chem.sc.edu.

(1) (a) Piguet, C.; Bernardinelli, G.; Hopfgartner, G. *Chem. Rev.* **1997**, *97*, 2005. (b) Hagrman, P. J.; Hagrman, D.; Zubieta, J. *Angew. Chem., Int. Ed.* **1999**, *38*, 2638. (c) Khlobystov, A. N.; Blake, A. J.; Champness, N. R.; Lemenovskii, D. A.; Majouga, G.; Zyk, N. V.; Schroder, M. *Coord. Chem. Rev.* **2001**, *222*, 155. (d) Blake, A. J.; Champness, N. R.; Hubberstey, P.; Li, W. S.; Withersby, M. A.; Schroder, M. *Coord Chem. Rev.* **1999**, *183*, 117. (e) Batten, S. T.; Robson, R. *Angew. Chem., Int. Ed.* **1998**, *37*, 1461. (f) Nguyen, P.; Gomez-Elipe, P.; Manners, I. *Chem. Rev.* **1999**, *99*, 1515. (g) Leininger, S.; Olenyuk, B.; Stang, P. J. *Chem. Rev.* **2000**, *100*, 853. (h) Swiegers, G. F.; Malefetse, T. J. *Chem. Rev.* **2000**, *100*, 3483. (i) Seidel, R. S.; Stang, P. J. *Acc. Chem. Res.* **2002**, *35*, 972. (j) Zaworotko, M. J. *Chem. Commun.* **2001**, 1.

(2) (a) Gardner, G. B.; Venkataraman, D.; Moore, J. S.; Lee, S. *Nature* **1995**, *374*, 792−793. (b) Venkataraman, D.; Gardner, G. B.; Lee, S.; Moore, J. S. *J. Am. Chem. Soc.* **1995**, *117*, 11600−11601. (c) Yaghi, O. M.; Li, G.; Li, H. *Nature* **1995**, *378*, 703−706. (d) Hennigar, T. J.; MacQuarrie, D. C.; Losier, P.; Rogers, R. D.; Zaworotko, M. J. *Angew. Chem., Int. Ed.* **1997**, *36*, 972. (e) Müller, I. M.; Röttgers, T.; Sheldrik, W. S. *Chem. Commun*. **1998**, 823. (f) Hong, M.; Zhao, Y.; Su, W.; Cao, R.; Fujita, M.; Zhou, Z.; Chan, A. S. C. *Angew. Chem., Int. Ed.* **2000**, *39*, 2468. (g) Blake, A. J.; Champness, N. R.; Cooke, P. A.; Nicolson, J. E. B. *Chem. Commun.* **2000**, 665.

(3) (a) Hirsch, K. A.; Wilson, S. R.; Moore, J. S. *Inorg. Chem.* **1997**, *36*, 2960. (b) Blake, A. J.; Champness, N. R.; Cooke, P. A.; Nicolson J. E. B.; Wilson C. *J. Chem. Soc., Dalton Trans*. **2000**, 3811. (c) Yang, S.-P.; Chen, X.-M.; Ji, L. *J. Chem. Soc., Dalton Trans*. **2000**, 2337. (d) Fei, B.-L.; Sun, W.-Y.; Yu, K-.B.; Tang, W.-X. *J. Chem. Soc., Dalton Trans*. **2000**, 805. (e) Paul, R. L.; S. M. Couchman, S. M.; Jeffery, J. C.; McCleverty, J. A.; Reeves, Z. R.; Ward, M. D. *J. Chem. Soc., Dalton Trans.*, **2000**, 845. (f) Carlucci, L.; Ciani, G.; Proserpio, D. M.; Rizzato, S. *CrystEngComm* **2002**, *4*, 121. (g) Plater, J. M.; Foreman, M. R. St. J.; Slawin, A. M. *J. Chem. Res., Synop*. **1999**, *74*. (h) Carlucci, L.; Ciani, G.; Proserpio, D. M.; Rizzato, S. *CrystEngComm* **2002**, *4*, 431.

(4) (a) Withersby, M. A.; Blake, A. J.; Champness, N. R.; Hubberstey, P.; Li, W.-S.; Schröder, M. *Angew. Chem., Int. Ed.* **1997**, *36*, 2327. (b) Vilar, R.; Mingos, D. M. P.; White, A. J. P.; Williams, D. J. *Angew. Chem., Int. Ed.* **1998**, *37*, 1258. (c) Hong, M. C.; Su, W. P.; Cao, R.; Fujita, M.; Lu, J. X. *Chem.—Eur. J.* **2000**, *6*, 427.

10.1021/ic7017743 CCC: $37.00
Published on Web 11/14/2007

Chart 1. $C_6H_{6-n}[CH_2OCH_2C(pz)_3]_n$ Family of Ligands

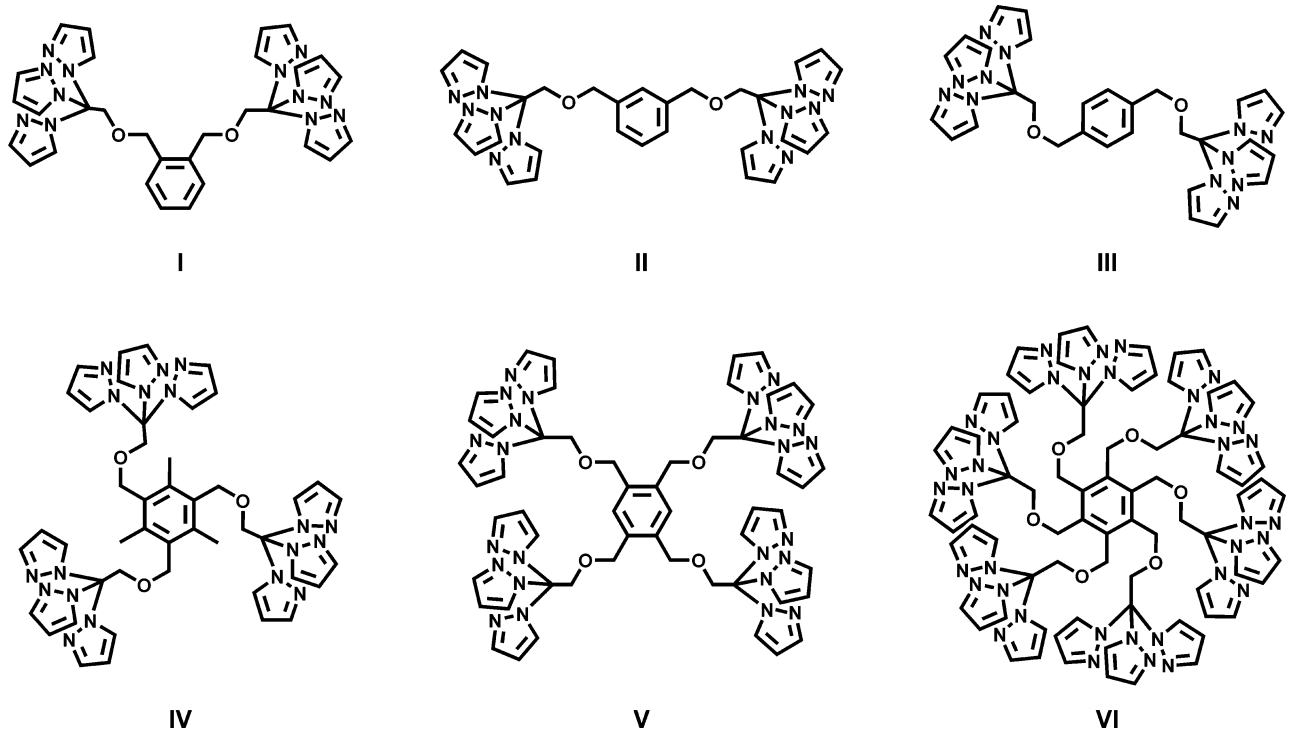

structures are strong[6] and weak[3e,7] hydrogen bonds, $\pi - \pi$ stacking,[8] X−H···π interactions (X = O, N, C),[9] and interhalogen interactions.[10]

We have recently studied metal complexes of multitopic ligands built from tris(1-pyrazolyl)methane units of the general formula $C_6H_{6-n}[CH_2OCH_2C(pz)_3]_n$ (n = 2, 3, 4, and 6, pz = pyrazolyl ring) (Chart 1) and showed that this donor set can act in different covalent binding modes as (a) κ^3 tripodal, (b) κ^2 bonded to a single metal with the third pyrazolyl ring not coordinated, and (c) $\kappa^2-\kappa^1$ bonded bridging two metals (Scheme 1).[11] These binding modes are mainly determined by the coordination preferences of the metal. For instance, in the case of a metal with octahedral

Scheme 1. Possible Modes of Coordination of Tris(1-pyrazolyl)methane Units

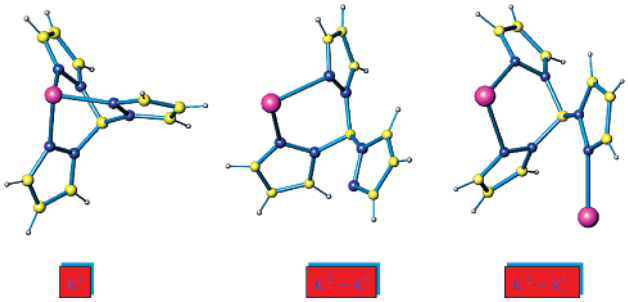

(5) (a) Withersby, M. A.; Blake, A. J.; Champness, N. R.; Cooke, Hubberstey, P. A., P.; Li, W.-S.; Schröder, M. *Inorg. Chem.* **1999**, *38*, 2259. (b) Subramanian, S.; Zaworotko, M. J. *Angew. Chem., Int. Ed*. **1995**, *34*, 2127. (c) Lu, J.; T. Paliwala, T.; Lim, S. C.; Yu, C.; Niu, T.; Jacobson, A. J. *Inorg. Chem.* **1997**, *36*, 923.

(6) Strong hydrogen bonds include interactions of the type O−H···O, N−H···O, O−H···N, and N−H···N. See for example: (a) Braga, D.; Grepioni, F. J. *Chem. Soc., Dalton Trans*. **1999**, 1. (b) Allen, M. T.; Burrows, A. D.; Mahon, M. F. *J. Chem. Soc., Dalton Trans*. **1999**, 215. (c) Ziener, U.; Breuning, E.; Lehn, J.-M.; Wegelius, E.; Rissanen, K.; Baum, G.; Fenske, D.; Vaughan, G. *Chem.—Eur. J*. **2000**, *6*, 4132. (d) Goddard, R.; Claramunt, R. M. Escolastico, C.; Elguero, J. *New. J. Chem.* **1999**, 237.

(7) A weak hydrogen bond (X−H···Y) involves less electronegative atoms; we discuss here only the C−H···Y type of weak hydrogen bond (Y = O, F). See for example: (a) Calhorda, M. J. *Chem. Commun*. **2000**, 801. (b) Desiraju, G. R. *Acc. Chem. Res.* **1996**, *29*, 441. (c) Grepioni, F.; Cojazzi, G.; Draper, S. M.; Scully, N.; Braga, D. *Organometallics* **1998**, *17*, 296. (d) Weiss, H. C.; Boese, R.; Smith, H. L.; Haley, M. M. *Chem. Commun*. **1997**, 2403.

(8) Janiak, C. *J. Chem. Soc., Dalton Trans*. **2000**, 3885 and references therein.

(9) (a) Takahashi, H.; Tsuboyama, S.; Umezawa, Y.; Honda, K.; Nishio, M. *Tetrahedron* **2000**, *56*, 6185. (b) Tsuzuki, S.; Honda, K.; Uchimaru, T.; Mikami, M.; Tanabe, K. *J. Am. Chem. Soc.* **2000**, *122*, 11450. (c) Seneque, O.; Giorgi, M.; Reinaud, O. *Chem. Commun*. **2001**, 984. (d) Weiss, H. C.; Blaser, D.; Boese, R.; Doughan, B. M.; Haley, M. M. *Chem. Commun*. **1997**, 1703. (e) Madhavi, N. N. L.; Katz, A. K.; Carrell, H. L.; Nangia, A.; Desiraju, G. R. *Chem. Commun*. **1997**, 2249. (f) Madhavi, N. N. L.; Katz, A. K.; Carrell, H. L.; Nangia, A.; Desiraju, G. R. *Chem. Commun*. **1997**, 1953. (g) Nishio, M.; Hirota, M.; Umezawa, Y. *The CH/π Interaction Evidence, Nature and Consequences*; Wiley-VCH: New York, 1998.

(10) (a) Reddy, D. S.; Craig, D. C.; Desiraju, G. R. *J. Am. Chem. Soc.* **1996**, 118, 4090. (b) Kowalik, J.; VanDerveer, D.; Clower, C.; Tolbert, L. M. *Chem. Commun*. **1999**, 2007. (c) Freytag, M.; Jones, P. G.; Ahrens, B.; Fischer, A. K. *New J. Chem*. **1999**, *23*, 1137. (d) Ram Thaimattam, R.; Reddy, D. S.; Xue, F.; Mak, T. C. W.; Nangia, A.; Desiraju, G. R. *New J. Chem*. **1998**, *22*, 143.

(11) (a) Reger, D. L.; Wright, T. D.; Semeniuc, R. F.; Grattan, T. C.; Smith, M. D. *Inorg. Chem.* **2001**, *40*, 6212. (b) Reger, D. L.; Semeniuc, R. F.; Smith, M. D. Inorg. Chem. **2001**, *40*, 6545. (c) Reger, D. L.; Semeniuc, R. F.; Smith, M. D. *Eur J. Inorg. Chem.* **2002**, 543. (d) Reger, D. L.; Semeniuc, R. F.; Smith, M. D. *J. Chem. Soc., Dalton Trans*. **2002**, 476. (e) Reger, D. L.; Semeniuc, R. F.; Smith, M. D. *Inorg. Chem. Commun*. **2002**, *5*, 278. (f) Reger, D. L.; Semeniuc, R. F.; Smith, M. D. *J. Organomet. Chem*. **2003**, *666*, 87. (g) Reger, D. L.; Semeniuc, R. F.; Smith, M. D. *J. Chem. Soc., Dalton Trans*. **2003**, 285. (h) Reger, D. L.; Semeniuc, R. F.; Silaghi-Dumitrescu, I.; Smith, M. D. *Inorg. Chem.* **2003**, *42*, 3751. (i) Reger, D. L.; Semeniuc, R. F.; Rassolov, V.; Smith, M. D. *Inorg. Chem.* **2004**, *43*, 537. (j) Reger, D. L.; Semeniuc, R. F.; Smith, M. D. *Inorg. Chem.* **2003**, *42*, 8137. (k) Reger, D. L.; Gardinier, J. R.; Semeniuc, R. F.; Smith, M. D. *J. Chem. Soc., Dalton Trans*. **2003**, 1712. (l) Reger, D. L.; Gardinier, J. R.; Smith, M. D. *Inorg. Chem.* **2004**, *43*, 3825.

preferences, like Cd(II)[11a] or $M(CO)_3$ (M = Mn, Re),[12] the κ^3 mode is observed. In the case of a metal with less defined coordination modes, like silver(I), the other two modes were encountered. To date, in the case of silver(I) chemistry, our most important findings about the self-assembly processes organizing these structures are that (a) the ligand usually displays a $\kappa^2-\kappa^1$ coordination mode of the $[C(pz)_3]$ units, but the $\kappa^2-\kappa^0$ mode was also found in some cases; (b) the "molecular" and supramolecular structures were dependent on the number of side arms and ligand topology, i.e., their position around the central arene ring; (c) the overall structures of the crystalline solids showed a dependency on both the counterion and the solvent; and (d) several different anions were involved in weak hydrogen bonds with the metal−organic−frameworks.

While most silver(I) complexes display the $\kappa^2-\kappa^1$ coordination mode, for ligands where the side arms are in close proximity, i.e., in the ortho-linked, bitopic ligand and 1,2,4,5 tetratopic ligand (I and V, Chart 1), the $\kappa^2-\kappa^0$ coordination mode was generally encountered.[11h] This result prompted our interest in answering the two following questions: (1) Is it possible to obtain the same type of architectures using a similar ligand that has only a bis(1-pyrazolyl)methane donor set, and (2) is it possible to use the "free" pyrazolyl ring in these $\kappa^2-\kappa^0$ tris(1-pyrazolyl)methane-based compounds to increase the dimensionality of the metal−organic framework from 1D to 2D? To answer the first question, we report here the synthesis of a new bis(1-pyrazolyl)methane-based ligand, o-$C_6H_4[CH_2OCH_2CH(pz)_2]_2$ (**L^2**) and its two silver(I) compounds, $\{o\text{-}C_6H_4[CH_2OCH_2CH(pz)_2]_2(AgPF_6)\}_n$ (**1**) and $\{o\text{-}C_6H_4[CH_2OCH_2CH(pz)_2]_2(AgO_3SCF_3)\}_n$ (**2**). In order to answer the second question, we report two new silver(I) compounds of the o-$C_6H_4[CH_2OCH_2C(pz)_3]_2$ (**L^3**) ligand,[11a] $\{o\text{-}C_6H_4[CH_2OCH_2C(pz)_3]_2(AgO_3SCF_3)\}_n$ (**3**) and $\{o\text{-}C_6H_4[CH_2OCH_2C(pz)_3]_2(AgO_3SCF_3)_2\}_n$ (**4**) respectively.

Experimental Section

General Procedure. All operations were carried out under a nitrogen atmosphere using standard Schlenk techniques and a Vacuum Atmospheres HE-493 drybox. All solvents were dried and distilled prior to use following standard techniques. The ^{1}H NMR spectra were recorded on a Varian AM300 spectrometer using a broad-band probe. Proton chemical shifts are reported in ppm and were referenced to undeuterated solvent signals (^{1}H) or deuterated solvent signals (^{13}C). Elemental analyses were performed by Robertson Microlit Laboratories (Madison, NJ). The ligand o-$C_6H_4[CH_2OCH_2C(pz)_3]_2$ (**L^3**) was prepared following the published method.[11a] Silver hexafluorophosphate, silver trifluoromethanesulfonate, dichloroacetic acid, pyrazole, and α,α′-dibromo-*o*-xylene were obtained from commercial sources (Aldrich) and used as received.

Synthesis of Bis(1-pyrazolyl)acetic acid, $(pz)_2CHCOOH$. Into a three-necked, 2 L flask, equipped with an overhead mechanical stirrer and a reflux condenser, pyrazole (48.0 g, 0.705 mol), KOH (52.0 g, 0.927 mol), K_2CO_3 (125 g, 0.904 mol), benzyltriethylammonium chloride (6.0 g, 0.026 mol), and 1.3 L of THF were added. To this suspension, dichloroacetic acid (30.0 g, 0.233 mol) was carefully added, and the third neck was stoppered. The system was heated at gentle reflux with vigorous stirring for 15 h and then allowed to cool to room temperature. The THF was removed in vacuo, and the remaining solid was dried in vacuo overnight. One liter of water was added to give a slightly cloudy, pale yellow solution. The solution was acidified to pH 7 by the careful addition of concentrated HCl and then washed with diethyl ether (3 × 200 mL) to remove unreacted pyrazole. The aqueous phase was then further acidified to pH 1. Upon brief agitation of this solution, 20.3 g of the pure desired product precipitated over approximately 30 min and was collected by suction filtration as a white crystalline solid that melted with decomposition at 163−164 °C (lit. 166 °C) and whose spectral characterization matched that of previous reports.[13] The remaining aqueous filtrate was extracted with a 2.5:1 diethyl ether/THF mixture (6 × 350 mL). The combined organic extracts were dried over $MgSO_4$, and the solvent was removed by rotary evaporation to yield a further 14.9 g of the crude product. Recrystallization of the crude material from a minimum amount of boiling acetone yielded 10.4 g of additional pure product. Total yield = 30.7 g (69%).

2,2′-Bis(1-pyrazolyl)ethanol, $(pz)_2CHCH_2OH$. To a 1 L volume of THF solution of bis(1-pyrazolyl)acetic acid (19.2 g, 0.100 mol) was added by cannula 100 mL of a 2.0 M, THF solution of $BH_3{\bullet}S(CH_3)_2$ (0.20 mol). The resulting solution was heated at reflux under N_2 for 22 h. After cooling to room temperature, the pH of the solution was reduced to 7 using half-concentrated acetic acid and allowed to stir at room temperature overnight. Water (200 mL) and diethyl ether (500 mL) were added, and the layers were separated. The aqueous phase was extracted with diethyl ether (3 × 50 mL), and the extracts, combined with the original organic phase, were washed with concentrated aqueous K_2CO_3. The organic phase was dried over $MgSO_4$ and filtered, and the solvent was removed by rotary evaporation to leave 12.5 g of the desired alcohol. Re-extraction of the aqueous phase with CH_2Cl_2 (4 × 100 mL), followed by drying over $MgSO_4$ yielded, after the removal of the solvent, an additional 2.7 g of product. Total yield = 15.2 g (85%). Mp: 99−102 °C. Anal. Calcd for $C_8H_{10}N_4O$: C, 53.92; H, 5.66; N, 31.44. Found: C, 53.85; H, 5.35; N, 31.04. IR (KBr, cm^{-1}): 3215, 3134, 3121, 3093, 2987, 2938, 2889, 1511, 1454, 1438. ^{1}H NMR ($CDCl_3$, 300 MHz): δ 7.62, 7.59 (d, d, J = 2.7 Hz, J = 1.8 Hz, 2 H, 2 H, 3,5-pz), 6.50 (t, J = 4.8 Hz, 1 H, C*H*(pz)$_2$), 6.31 (t, J = 2.3 Hz, 2 H, 4-pz), 4.51 (d, J = 4.5 Hz, 2 H, C*H*$_2$OH), 3.36 (br s, 1 H, CH$_2$O*H*). ^{13}C NMR ($CDCl_3$, 75.5 MHz): δ 140.2, 129.5, 106.8, 74.6, 63.3. MS direct probe *m*/*z* (rel. % abund.) [assgn]: 178 (2) $[M]^+$, 147 (100) $[M - CH_2OH]^+$, 111 (15) $[M - pz]^+$.

Synthesis of o-$C_6H_4[CH_2OCH_2CH(pz)_2]_2$ (L^2). To a suspension of NaH (0.052 g, 2.20 mmol) in 50 mL of dry THF 2,2′-bis(1-pyrazolyl)ethanol (0.339 g, 2.18 mmol) was added. When the mixture turned transparent (ca. 30 min), α,α′-dibromo-*o*-xylene (0.288 g, 1.09 mmol) was added. The reaction was heated at reflux for 16 h, during which a white precipitate formed. The suspension was allowed to cool, and 100 mL of H_2O was added. The solution was extracted with dichloromethane (3 × 100 mL). The combined organic layer was dried with $MgSO_4$ and filtered. The solvent was removed in vacuo to give a pale yellow oil. This oil was dissolved in 5 mL of dichloromethane, and 25 mL of distilled hexanes was added to the solution to produce a white precipitate. The dichloromethane/hexanes mixture was evaporated to give an off-white solid. This solid was triturated with hexanes until a white powder formed. The suspension was filtered and allowed to dry to afford

(12) (a) Reger, D. L.; Semeniuc, R. F.; Smith, M. D. *J. Chem. Soc., Dalton Trans.* **2002**, 476. (b) Reger, D. L.; Brown, K. J.; Smith, M. D. *J. Organomet. Chem.* **2002**, *658*, 50.

(13) Burzlaff, N.; Hegelmann, I.; Weibert, B. *J. Organomet Chem.* **2001**, *626*, 16.

the desired product. Yield: 0.309 g (62%). Mp: 83−85 °C. Anal. Calcd for $C_{24}H_{26}N_8O_2$: C, 62.87; H, 5.72; N, 24.44. Found: C, 62.64; H, 5.71; N, 23.35. ^{1}H NMR (acetone-d_6, 300 MHz): δ 7.88, 7.51 (d, d, J = 2.4 Hz, J = 1.6 Hz, 4 H, 4 H, 3,5-pz), 7.26 (m, 4 H, arene) 6.83 (t, J = 6.9 Hz, 2 H, C*H*(pz)$_2$), 6.29 (t, J = 2.1 Hz, 4 H, 4-pz), 4.51 (s, 4 H, ArCH_2), 4.42 (d, J = 6.9 Hz, 4 H, OCH_2-CH). ^{1}H NMR (acetonitrile-d_3, 300 MHz): δ 7.78, 7.52 (d, d, J = 2.7 Hz, J = 1.5 Hz, 4 H, 4 H, 3,5-pz), 7.26 (m, 4 H, arene), 6.70 (t, J = 6.6 Hz, 2 H, C*H*(pz)$_2$), 6.30 (t, J = 2.1 Hz, 4 H, 4-pz), 4.47 (s, 4 H, ArCH_2), 4.39 (d, J = 6.6 Hz, 4 H, OCH_2CH). ^{13}C NMR (acetonitrile-d_6, 75.5 MHz): δ 141.0 (pz), 137.1 (arene), 130.2 (arene), 129.8 (pz), 128.9 (arene), 107.2 (pz), 74.5, 71.4, 70.1. MS ESI(+) *m*/*z* (rel. % abund.) [assgn]: 481 (97) [**L²** + Na]$^+$, 459 (100) [**L²**+ H]$^+$, 391 (30) [**L²** − pz]$^+$. HRMS: ES$^+$ (*m*/*z*): [**L²** + H]$^+$ calcd for $C_{24}H_{27}N_8O_2$ 459.2257; found 459.2251.

Synthesis of {*o*-C$_6$H$_4$[CH$_2$OCH$_2$CH(pz)$_2$]$_2$(AgPF$_6$)}$_n$ (1). The ligand **L²** (0.229 g, 0.50 mmol) was dissolved in 50 mL of dry THF, and silver hexafluorophosphate (0.126 g, 0.50 mmol) was added. The reaction was stirred for 16 h, and a white precipitate formed. The system was cannula filtered and the solid was washed with 10 mL of THF. The remaining solid was vacuum-dried at 100 °C, which give a white solid as the desired product. Yield: 0.271 g (76%). Anal. Calcd for $C_{24}H_{26}N_8O_2AgPF_6$: C, 40.52; H, 3.68; N, 15.75. Found: C, 40.25; H, 3.59; N, 15.46. ^{1}H NMR (acetone-d_6, 300 MHz): δ 8.17, 7.86 (s, s, 4 H, 4 H, 3,5-pz), 7.34 (t, J = 7.8 Hz, 2 H, C*H*(pz)$_2$), 7.21 (m, 4 H, arene), 6.50 (s, 4 H, 4-pz), 4.93 (d, J = 7.8 Hz, 4 H, OCH_2CH), 4.30 (s, 4 H, ArCH_2). ^{1}H NMR (acetonitrile-d_3, 300 MHz): δ 7.83, 7.64 (d, d, J = 2.1 Hz, J = 1.8 Hz, 4 H, 4 H, 3,5-pz), 7.24 (m, 2 H, arene), 7.19 (m, 2 H, arene) 6.77 (t, J = 7.5 Hz, 2 H, C*H*(pz)$_2$), 6.36 (t, J = 2.1 Hz, 4 H, 4-pz), 4.47 (d, J = 7.5 4 H, OCH_2CH), 4.28 (s, 4 H, ArCH_2). ^{13}C NMR (acetonitrile-d_6, 75.5 MHz): δ 143.0 (pz), 137.2 (arene), 132.4 (arene), 130.8 (pz), 129.4 (arene), 107.6 (pz), 73.6, 72.2, 70.2. MS ESI(+) *m*/*z* (rel. % abund.) [assgn]: 565 (90) [**L²**Ag]$^+$. HRMS: ES$^+$ (*m*/*z*): [**L²**Ag]$^+$ calcd for [$C_{24}H_{26}N_8O_2$Ag]$^+$ 565.1230; found 565.1230.

Synthesis of {*o*-C$_6$H$_4$[CH$_2$OCH$_2$CH(pz)$_2$]$_2$(AgO$_3$SCF$_3$)}$_n$ (2). The ligand **L²** (0.070 g, 0.153 mmol) was dissolved in 50 mL of dry THF, and silver trifluoromethanesulfonate (0.039 g, 0.153 mmol) was added. The reaction was stirred for 17 h, and a white precipitate formed. The system was cannula filtered, and the solid was washed with 10 mL of THF. The solvent was removed to give a white solid. After the solid was dried for 4 days under vacuum, ^{1}H NMR analysis indicated pure product. Yield = 0.050 g (46%). Anal. Calcd for $C_{25}H_{26}N_8O_5AgF_3S$: C, 41.97; H, 3.66; N, 15.66. Found: C, 42.33; H, 3.73; N, 15.47. ^{1}H NMR (acetone-d_6, 300 MHz): δ 8.20, 7.85 (s, s, 4 H, 4 H, 3,5-pz), 7.37 (t, J = 7.5 Hz, 2 H, C*H*(pz)$_2$) 7.20 (m, 4 H, arene), 6.49 (s, 4 H, 4-pz), 4.90 (d, J = 7.5, 4 H, OCH_2CH), 4.32 (s, 4 H, ArCH_2). ^{1}H NMR (acetonitrile-d_3, 300 MHz): δ 7.87, 7.71 (d, d, J = 2.7 Hz, J = 2.1 Hz, 4 H, 4 H, 3,5-pz), 7.25 (m, 2 H, arene), 7.17 (m, 2 H, arene) 6.83 (t, J = 7.2 Hz, 2 H, C*H*(pz)$_2$), 6.39 (t, J = 1.8 Hz, 4 H, 4-pz), 4.52 (d, J = 7.2 Hz, 4 H, OCH_2CH), 4.20 (s, 4 H, ArCH_2). ^{13}C NMR (acetonitrile-d$_6$, 75.5 MHz): δ 143.0 (pz), 137.2 (arene), 132.5 (arene), 130.8 (pz), 129.4 (arene), 107.6 (pz), 73.5, 72.1, 70.2. MS ESI(+) *m*/*z* (rel. % abund.) [assgn]: 565 (100) [**L²**Ag]$^+$. HRMS: ES$^+$ (*m*/*z*): [**L²**Ag]$^+$ calcd for [$C_{24}H_{26}N_8O_2$Ag]$^+$ 565.1230; found 565.1224.

Synthesis of {*o*-C$_6$H$_4$[CH$_2$OCH$_2$C(pz)$_3$]$_2$(AgO$_3$SCF$_3$)}$_n$ (3). *o*-C$_6$H$_4$[CH$_2$OCH$_2$C(pz)$_3$]$_2$, **L³**, (0.147 g, 0.25 mmol) was dissolved in THF (20 mL). This solution was added dropwise to a solution of silver trifluoromethanesulfonate (0.064 g, 0.25 mmol) in dry THF (10 mL) under an inert atmosphere. A white precipitate appeared as the mixture and was stirred for 1 h. The THF was removed by cannula filtration, and the white precipitate washed with THF (2 × 10 mL) and then vacuum-dried to afford 0.226 g (74%) of solid identified as {*o*-C$_6$H$_4$[CH$_2$OCH$_2$C(pz)$_3$]$_2$(AgO$_3$SCF$_3$)}$_n$ (**3**). Anal. Calcd for $C_{31}H_{30}AgF_3N_{12}O_5S$: C, 43.93; H, 3.57. Found: C, 44.31; H, 3.48. ^{1}H NMR (acetone-d_6): δ 7.88, 7.60 (d, d, J = 1.5 and J = 2.7 Hz, 6 H, 6 H, 3,5-pz), 7.27 (m, 4 H, arene), 6.55 (dd, J = 1.7 and 2.7 Hz, 6 H, 4-pz), 5.23 (s, 4 H, OCH_2C(pz)$_3$), 4.55 (s, 4 H, ArCH_2). ES$^+$/MS: [**L³**Ag]$^+$ calcd for [$C_{30}H_{30}N_{12}O_2$Ag]$^+$ 697.1666; found 697.1677.

Synthesis of {*o*-C$_6$H$_4$[CH$_2$OCH$_2$C(pz)$_3$]$_2$(AgO$_3$SCF$_3$)$_2$}$_n$·solvate (4·solv). 5 mg of **L³** was dissolved in 4 mL of acetone. To this solution was added 3 equiv of AgO_3SCF_3. This solution was inserted in a small test tube via a pipet. The open small test tube was inserted in a second one that already had ca. 50 mL of diethyl ether and closed with a Teflon screw cap. The test tubes were kept at room temperature for several days, during which time colorless crystals of **4**·solv grew.

Crystallography. X-ray diffraction intensity data for each compound were measured at 150 K using a Bruker SMART APEX diffractometer (Mo Kα radiation, λ = 0.71073 Å).[14] The raw area detector data frames were processed with *SAINT*+.[14] The reported unit cell parameters were determined by least-squares refinement of strong reflections taken from each data set (6197 for **1**·2[$(CH_3)_2$CO], 6105 for **2**·1.5[$(CH_3)_2$CO], 7451 for **3**, and 8989 for **4**·solv). Direct methods structure solutions (except for **3**, solved by Patterson methods), difference Fourier calculations, and full-matrix least-squares refinements against F^2 were performed with the *SHELXTL* software package.[15] All non-hydrogen atoms were refined with anisotropic displacement parameters except where noted (**4**·solv). Hydrogen atoms were placed in geometrically idealized positions and included as riding atoms. Information regarding the structure solution and refinement for each structure is given below, and the numerical results are given in Table 1.

Compound **1**·2[$(CH_3)_2$CO] crystallizes in the triclinic system. The space group $P\bar{1}$ was confirmed by the successful solution and refinement of the data. The asymmetric unit consists of one Ag atom, one $C_{24}H_{26}N_8O_2$ ligand, one PF_6^- anion, and two acetone molecules.

Compound **2**·1.5[$(CH_3)_2$CO] crystallizes in the space group $P2_1/m$ as determined by the pattern of systematic absences in the intensity data and by obtaining a reasonable structure solution and refinement. The asymmetric unit consists of one Ag atom, one $C_{24}H_{26}N_8O_2$ ligand, half each of two independent $CF_3SO_3^-$ anions, and 1.5 independent acetone molecules.

Compound **3** crystallizes in the triclinic system. Intensity statistics strongly indicated an acentric structure. The space group $P1$ (No. 1) was confirmed over $P\bar{1}$ (No. 2) by obtaining a reasonable and stable structure solution and refinement, by inspection of the structure, and by checking for missed symmetry elements with the *ADDSYM* program in *PLATON*.[16] At convergence, the absolute structure (Flack) parameter was 0.00(2), indicating the correct absolute structure and the absence of racemic twinning. There is one Ag atom, one $C_{24}H_{26}N_8O_2$ ligand, and one triflate ion in the asymmetric unit.

Compound **4**·solv crystallizes in the space group $P2_1/c$. Initial solution and refinement proceeded smoothly, yielding four in-

(14) *SMART*, version 5.625, *SAINT*+, version 6.45; Bruker Analytical X-ray Systems, Inc.: Madison, WI, 2001.
(15) *SHELXTL*, version 6.14; Bruker Analytical X-ray Systems, Inc.: Madison, WI, 2000.
(16) *PLATON*: (a) Spek, A. L. *Acta Crystallogr., Sect. A* **1990**, *46*, C34. (b) Spek, A. L. *PLATON, A Multipurpose Crystallographic Tool*; Utrecht University: Utrecht, The Netherlands, 2002.

Table 1. Selected Crystal and Structure Refinement Data

	1·2[$(CH_3)_2CO$]	**2**·1.5[$(CH_3)_2CO$]	**3**	**4**·solv
formula	$C_{30}H_{38}AgF_6N_8O_4P$	$C_{29.5}H_{35}AgF_3N_8O_{6.5}S$	$C_{31}H_{30}AgF_3N_{12}O_5S$	$C_{72}H_{81}Ag_4F_9N_{24}O_{15.5}S_3$
fw, g mol^{-1}	827.52	802.59	847.60	2229.27
cryst syst	triclinic	monoclinic	triclinic	monoclinic
space group	$P\bar{1}$	$P2_1/m$	$P1$ (No. 1)	$P2_1/c$
T, K	150(1)	150(1)	150(1)	150(1)
a, Å	9.0715(4)	9.0339(3)	8.2566(5)	13.5708(6)
b, Å	13.5523(6)	26.995(1)	10.3960(6)	28.5556(12)
c, Å	14.9505(6) Å	15.3334(6)	10.4792(6)	25.5868(11)
α, deg	84.728(1)	90	95.528(1)	90
β, deg	88.297(1)	92.521(1)	91.541(1)	101.854(1)
γ, deg	83.173(1)	90	106.084(1)	90
V, Å^3	1816.93(13)	3735.8(2)	858.91(9)	9704.0(7)
Z	2	4	1	4
R_1 ($I > 2\sigma(I)$)	0.0428	0.0481	0.0494	0.0818
wR_2 ($I > 2\sigma(I)$)	0.1151	0.1451	0.1198	0.2071

Scheme 2. Synthesis of $\mathbf{L^2}$

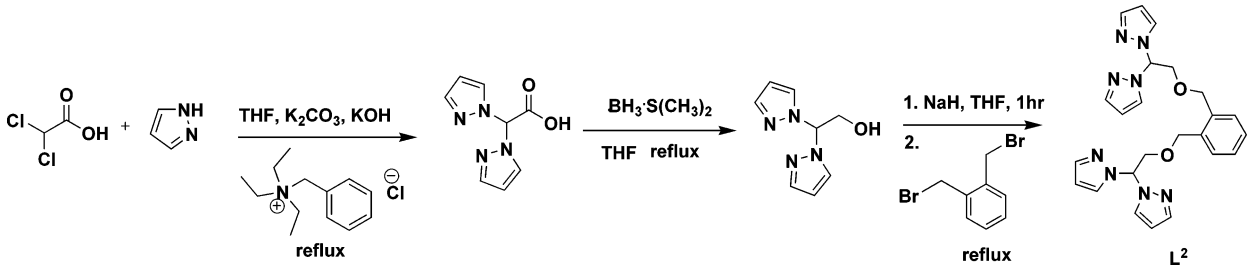

equivalent Ag positions, two independent *o*-$C_{30}H_{30}N_{12}O_2$ ligands, and three of the four expected triflate counterions. One of the located triflates is disordered over two positions near Ag4 in a 65:35 ratio. All atoms of these framework species were refined anisotropically. Location and refinement of the remaining contents of the asymmetric unit was hampered by high solvent content and accompanying extensive solvent/anion disorder. The nonframework volume in the unit cell was calculated to be 2881.3 Å^3 or 29.7% of the total unit cell volume of 9704.0 Å^3.[16] Within this volume, one acetone molecule, one Et_2O molecule disordered over two general positions, and half of another Et_2O molecule disordered about an inversion center could be reasonably refined with the use of several restraints. The acetone is disordered over four sites about a center of symmetry and was refined anisotropically without incident. Both disordered Et_2O molecules were refined with an isotropic displacement parameter common to each unit. In total, 93 restraints (SHELX DFIX, DANG, and SAME instructions) were used in modeling the anion/triflate disorder. The fourth triflate ion could not be reliably located nor could reasonable disorder models be assigned to the many remaining electron density peaks. This diffuse region was therefore treated with *SQUEEZE*.[16] The program removed the contribution of the disordered species in the remaining 1223.2 Å^3 volume (455 e$^-$/cell) from the structure factors. The tabulated fw, *d*(calc), and *F*(000) values reflect known unit cell contents only. After the final refinement cycle, large residual electron density peaks (2.2, 3.8, 5.0, and 5.9 e$^-$/Å^3) remain near the four Ag atoms. This is probably an artifact of contamination from a small crystallite or unrecognized twinning associated with the data crystal.

Results

Syntheses and Characterization. The $\mathbf{L^3}$ ligand was prepared as described earlier.[11a] The ligand $\mathbf{L^2}$ was synthesized as shown in Scheme 2. A procedure reported by Burzlaff to make bis(1-pyrazoyl)acetic acid from dibromoacetic acid and pyrazole[13] has been modified to make bis(1-pyrazoyl)acetic acid in better yields by using dichloroacetic acid instead of dibromoacetic acid. The bis(1-pyrazoyl)acetic acid is reduced using borane dimethyl sulfide complex to give 2,2-bis(1-pyrazoyl)ethanol in good yield. The 2,2-bis(1-pyrazoyl)ethanol is added to a suspension of NaH to form the alkoxide in situ. To this solution, α,α′-dibromo-*o*-xylene is added to give the desired ligand $\mathbf{L^2}$.

The preparations of **1**−**3** were readily achieved by combining equal molar amounts of the ligands with either $AgPF_6$ or AgO_3SCF_3. These compounds (insoluble in halogenated solvents, water, or alcohols but soluble in acetone, acetonitrile, and nitromethane) are white solids that are air-stable and show only slight decomposition after several weeks of exposure to daylight. A few crystals of solvated $\{o\text{-}C_6H_4[CH_2OCH_2C(pz)_3]_2(AgO_3SCF_3)_2\}_n$ (**4**·solv) were isolated by vapor-phase diffusion of diethyl ether into an acetonitrile solution of a 3/1 mixture of AgO_3SCF_3 and *o*-$C_6H_4[CH_2OCH_2C(pz)_3]_2$. Attempts to isolate compound **4** in its bulk form from a reaction similar to the preparations of **1**−**3** failed.

The ^{1}H NMR spectra of the silver(I) complexes **1** and **2** in acetonitrile are clearly different from those of the free ligands, showing that this strongly coordinating solvent does not displace the bis(1-pyrazolyl)methane units from coordination to silver(I). As previously observed with other silver(I) complexes,[11] acetonitrile completely replaces the ligands in the tris(1-pyrazolyl)methane-based complexes **3** and **4**·solv; the spectra of these compounds in CD_3CN are the same as those of the free ligands in this solvent. The ^{1}H spectra of all these compounds in deuterated acetone are different from the free ligands, showing the coordination of both types of ligands to the silver(I) in this solution. Interestingly, the ^{1}H NMR spectrum of **4**·solv in acetone is identical with that of **3**, indicating **4**·solv dissociates into **3** and free AgO_3SCF_3

Table 2. Selected Bond Distances (Å) and Angles (deg) for **1**·2[$(CH_3)_2CO$], **2**·1.5[$(CH_3)_2CO$], and **3**

	1·2[$(CH_3)_2CO$]	**2**·1.5[$(CH_3)_2CO$]	**3**
	Bond Distances		
Ag−N(11)	2.347(3)	2.335(3)	2.313(5)
Ag−N(21)	2.269(2)	2.269(3)	2.373(3)
Ag−N(31*)	2.281(2)	2.326(3)	
Ag−N(41*)	2.341(2)	2.290(3)	2.340(4)
Ag−N(51*)			2.517(5)
	Bond Angles		
N(11)−Ag−N(21)	83.75(8)	84.05(10)	79.46(16)
N(11)−Ag−N(31*)	131.50(9)	127.20(10)	
N(11)−Ag−N(41*)	113.49(8)	120.20(10)	157.76(15)
N(11)−Ag−N(51*)			97.62(15)
N(21)−Ag−N(31*)	120.95(8)	115.29(9)	
N(21)−Ag−N(41*)	127.75(8)	130.11(9)	108.55(17)
N(21)−Ag−N(51*)			165.18(15)
N(31*)−Ag−N(41*)	85.01(8)	85.46(9)	
N(41*)−Ag−N(51*)			79.60(16)

Table 3. Selected Bond Distances (Å) and Angles (deg) for **4**·solv

Bond distances		Bond angles	
Ag(1)−N(11)	2.326(5)	N(11)−Ag(1)−N(21)	80.75(18)
Ag(1)−N(21)	2.279(5)	N(11)−Ag(1)−N(101*)	135.10(19)
Ag(1)−N(101*)	2.296(5)	N(11)−Ag(1)−N(111*)	119.7(2)
Ag(1)−N(111*)	2.307(6)	N(21)−Ag(1)-N(101*)	125.74(19)
Ag(2)−N(41)	2.245(5)	N(21)−Ag(1)−N(111*)	120.66(19)
Ag(2)−N(51)	2.367(5)	N(101*)−Ag(1)−N(111*)	80.37(18)
Ag(2)−N(72)	2.362(6)	N(41)−Ag(2)−N(51)	81.95(18)
Ag(2)−N(82)	2.262(5)	N(41)−Ag(2)−N(72)	126.2(2)
Ag(3)−N(61**)	2.273(6)	N(41)−Ag(2)−N(82)	141.4(2)
Ag(3)−N(121)	2.283(5)	N(51)−Ag(2)−N(72)	104.13(19)
Ag(3)−O(11)	2.404(5)	N(51)−Ag(2)−N(82)	119.78(19)
Ag(3)−O(21)	2.421(5)	N(72)−Ag(2)−N(82)	81.88(19)
Ag(4)−N(31)	2.163(5)	N(61**)−Ag(3)−N(121)	120.7(2)
Ag(4)−N(91***)	2.165(6)	N(61**)−Ag(3)−O(11)	85.35(19)
Ag(4)−O(31A***)	2.401(12)	N(61**)−Ag(3)−O(21)	138.29(18)
		N(121)−Ag(3)−O(11)	131.87(17)
		N(121)−Ag(3)−O(21)	88.69(17)
		O(11)−Ag(3)−O(21)	96.40(19)
		N(31)−Ag(4)−N(91***)	153.1(2)
		N(31)−Ag(4)−O(31A***)	116.8(4)
		N(91***)−Ag(4)−O(31A***)	89.5(4)

in solution. For all complexes, although the X-ray structures show that in the solid state the pyrazolyl rings are nonequivalent (vide infra), the NMR spectra show equivalent rings, presumably because of fast exchange of the ligands on the NMR time scale. As observed previously with tris(1-pyrazolyl)methanesilver(I) complexes of the $C_6H_{6-n}[CH_2OCH_2C(pz)_3]_n$ ligands with different counterions, the spectra of **1** and **2** are essentially identical. This result suggests that the cationic species present in solution are anion independent.

Solid-State Structures. Crystallization experiments were performed for all complexes by vapor-phase diffusion of diethyl ether into an acetone solution of the compound. Significant bond lengths and angles are listed in Tables 2 and 3.

Crystal Structure of $\{o\text{-}C_6H_4[CH_2OCH_2CH(pz)_2]_2\text{-}(AgPF_6)\cdot 2[(CH_3)_2CO]\}_n$ (1·2[$(CH_3)_2CO$]). The asymmetric unit consists of one Ag atom, one $\mathbf{L^2}$ ligand (Figure 1), one PF_6^- anion, and two acetone molecules. Two pyrazolyl rings from two different ligands chelate the silver atoms in a distorted-tetrahedral arrangement that is strongly influenced by the "bite" angle of the bis(1-pyrazolyl)methane unit. The restraints imposed by the bite angles of the ligands lower the N(11)−Ag−N(21) and N(41)−Ag−N(51) angles to

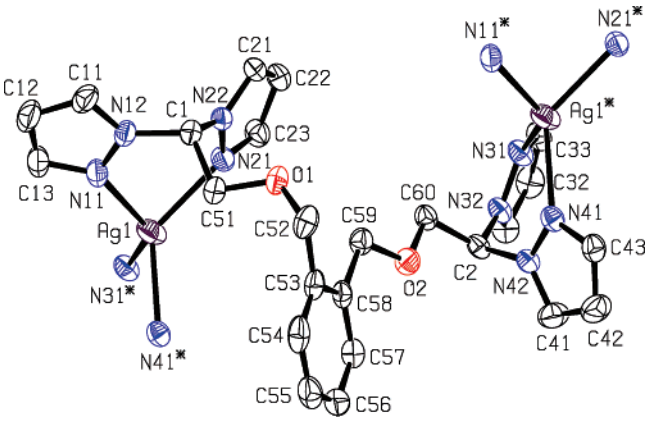

Figure 1. ORTEP diagram of repeating cationic unit in **1**·2[$(CH_3)_2CO$]. Displacement parameters are drawn at the 50% probability level. Hydrogen atoms and some atom labels are omitted for clarity.

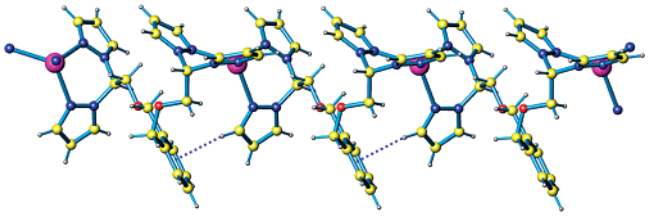

Figure 2. One strand of **1**·2[$(CH_3)_2CO$], showing the CH···π interaction between a pyrazolyl ring and the central arene ring as a blue dotted line. Color code: silver, purple; carbon, yellow; oxygen, red; nitrogen, blue.

83.75(8)° and 85.01(8)°, respectively. The nitrogen−silver bond lengths are within the normal range for these types of compounds (see Table 2).[11]

The bitopic nature of the ligand, combined with the opposite orientation of the chelating vectors (vector from center of the N···N donor atom distance to silver) of the bis(1-pyrazolyl) moiety generate a linear 1D coordination polymer, with the strands running along the *a* axis of the unit cell (Figure 2). One of the side arms (CH_2−O−CH_2 set of atoms) lies in the same plane with the central arene ring, while the other is bent out of the plane. The central arene rings are situated on the same side of the polymeric chain. This structural feature of the strand is supported by a CH···π interaction between the H(43) atom from a pyrazolyl ring and the central arene ring, as pictured in Figure 2 by the blue dotted lines. The H−centroid distance is 2.55 Å (C−centroid distance = 3.59 Å), and the corresponding C−H−centroid angle is 148°.

Two such strands are interdigitated (Figure 3) and held together by a CH···π interaction involving the CH_2 group next to the arene ring and an arene ring from a second, adjacent strand, with a H−centroid distance of 2.51 Å (C−centroid distance = 3.45 Å) and a C−H−arene ring angle of 158°, as pictured in Figure 3 by the red dotted lines. In addition, there is a second CH···π interaction between the H(55) atom situated on the central arene ring and a pyrazolyl ring from an adjacent strand, also pictured by red dotted lines in Figure 3. The H−centroid distance is 2.78 Å (C−centroid distance = 3.68 Å), and the corresponding C−H−centroid angle is 161°. The distance between the silver atoms within the strand is 9.07 Å, and the distance between the strands is 9.68 Å. The corresponding Ag−Ag−Ag angles are 86.42°

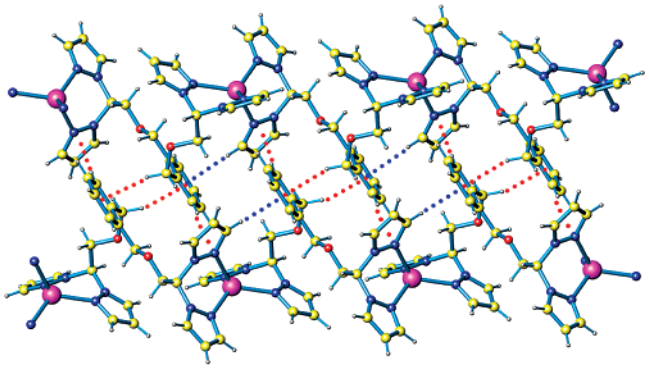

Figure 3. Two interdigitated strands of **1**·2[$(CH_3)_2CO$]; the red dotted lines show the two types of interstrand CH···π interactions, and the blue dotted lines show the intrastrand CH···π interactions, also pictured in Figure 2.

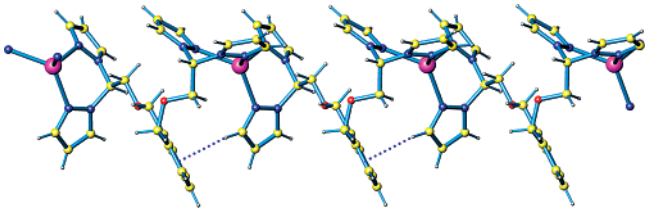

Figure 4. One strand of **2**·1.5[$(CH_3)_2CO$]); note the similarity between this strand and the covalent network of **1**·2[$(CH_3)_2CO$].

and 93.57°, respectively, defining a parallelogram. The PF_6^- anions and the acetone molecules of crystallization are situated along the strands, with no significant supramolecular interactions between these species and the dimeric strands.

Crystal Structure of {*o*-C_6H_4[$CH_2OCH_2CH(pz)_2$]$_2$-(AgO_3SCF_3)·1.5[$(CH_3)_2CO$]}$_n$ (2·1.5[$(CH_3)_2CO$]). This compound crystallizes in the space group $P2_1/m$, and its asymmetric unit consists of one Ag atom, one **L²** ligand, half each of two independent $CF_3SO_3^-$ anions, and 1.5 independent acetone molecules. Its structural characteristics, shown in Figure 4, are extremely similar to those of **1**·2[$(CH_3)_2CO$]; the numbering scheme is the same as that shown in Figure 1. There is the same distorted-tetrahedral arrangement around the metallic center, with the chelate N(11)−Ag−N(21) and N(31)−Ag−N(41) angles being 84.05(10)° and 85.46(9)°, respectively. It also forms a linear 1D strand, supported by a similar CH···π interaction between the H(43) atom from a pyrazolyl ring and the central arene ring. The H−centroid distance is 2.56 Å (C−centroid distance = 3.41 Å), and the corresponding C−H−centroid angle is 150°. The interdigitation of two strands is also similar and supported by analogous CH···π interactions, involving the CH_2 group next to the arene ring and a arene ring from a second, adjacent strand, and another between the H(55) situated on the central arene ring and a pyrazolyl ring from an adjacent strand, as pictured in Figure 3 for compound **1**·2[$(CH_3)_2CO$]. The geometrical characteristics of these two interactions are as follows: For the first interaction, the H−centroid distance is 2.48 Å (C−centroid distance is 3.44 Å) and the C−H−arene ring angle is 162°. For the second CH···π interaction, the H−centroid distance is 2.86 Å (C−centroid distance is 3.78 Å) and the corresponding C−H−centroid angle is 164°.

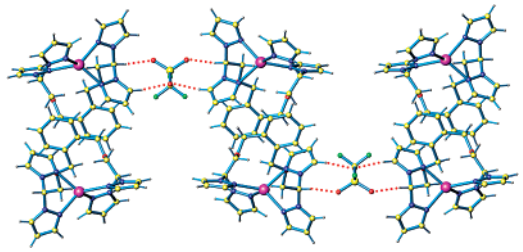

Figure 5. The hydrogen-bonding behavior of the triflate anion in **2**·1.5-[$(CH_3)_2CO$] forming corrugated supramolecular sheets.

In addition, due to the better hydrogen-bonding properties of the triflate anion in comparison with the PF_6^- moiety, these dimeric strands are associated into corrugated sheets. Each triflate anion is involved in a series of interactions, as can be seen in Figure 5 (red dotted lines). One oxygen atom, O(12A), situated on a mirror plane, forms a bifurcated hydrogen bond with the acidic H(41) atom from a pyrazolyl ring; the O−H distance is 2.35 Å (O−C distance is 3.29 Å), and the corresponding C−H−O angle is 171°. The remaining oxygen atoms, related by a mirror plane, form a pair of interactions with the hydrogen atoms from the [$HC(pz)_2$] donor set: The O−H distance is 2.30 Å (O−C distance is 3.27 Å), and the corresponding C−H−O angle is 167°. The sum of these interactions built up the corrugated sheets pictured in Figure 5, with the acetone molecules of crystallization (omitted for clarity) situated between the dimeric strands, next to the triflate anions.

Crystal Structure of 3. The presence of a third pyrazolyl ring in the poly(1-pyrazolyl)methane units generates significant differences in the solid-state structure of the compound, although there are many similarities as well. As can be seen in Figure 6, each silver atom is κ^2-bonded to two tris(1-pyrazolyl)methane units from two different ligands, with each unit having one pyrazolyl ring that is not coordinated to a silver atom.

The silver atom is in a distorted geometry between that of tetrahedral and square planar. In addition to the restraints imposed by the bite angle of the tris(1-pyrazolyl)methane unit lowering the angles N(11)−Ag−N(21) and N(41*)−Ag−N(51*) to 79.46(16)° and 79.60(16)°, respectively (Table 2), two of the interligand angles are 157.76(15)° and 165.18(15)°, approaching the square-planar angle of 180°.

Each bitopic ligand bonds two silver atoms in this $\kappa^2-\kappa^0$ fashion, forming a 1D polymer chain (Figure 7). The noncoordinated pyrazolyl rings, one from each unit, are oriented away from the strand. The central arene rings are situated on the same side of the polymeric chain, as in compounds **1** and **2**. Half of the noncoordinated pyrazolyl rings are oriented toward a methylene group adjacent to the central arene ring. This orientation is supported by a C−H···π interaction (pictured as blue dotted lines in Figure 7) between this pyrazolyl ring and one hydrogen atom from the methylene group, with a H(71b)−centroid distance of 2.73 Å, the C(71)−centroid distance of 3.46 Å, and the corresponding C−H−centroid angle of 131°.

The triflate anions are situated along the chain, being involved in hydrogen bonds with acidic hydrogen atoms (red

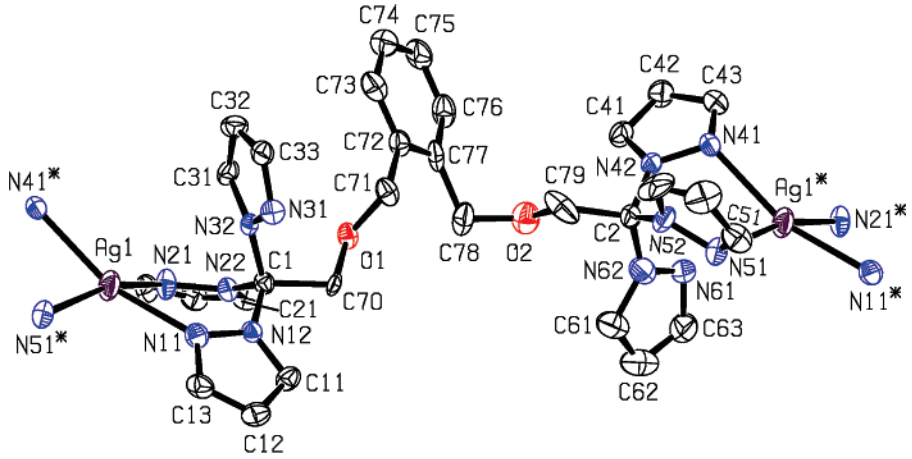

Figure 6. ORTEP diagram of repeating cationic unit in **3**. An asterisk indicates a symmetry-equivalent atom. Displacement parameters are drawn at the 40% probability level. Hydrogen atoms and some atom labels are omitted for clarity.

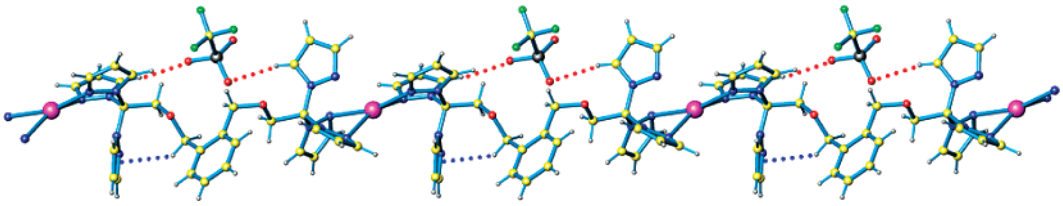

Figure 7. One strand of **3**, showing the CH···π interaction between a pyrazolyl ring and one hydrogen atom from the methylene group as blue dotted lines and the hydrogen-bonding behavior of the triflate anion as red dotted lines. Color code: same as that in Figure 2.

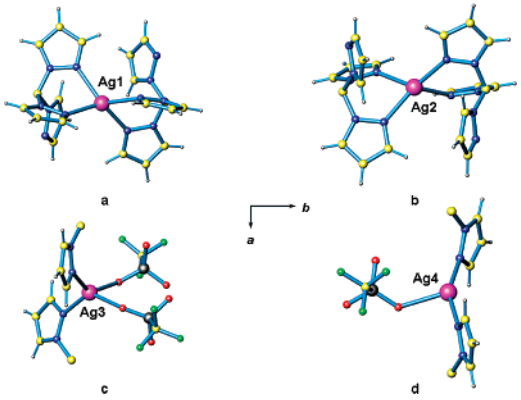

Figure 8. Coordination environment for the four independent silver atoms in **4**·solv.

dotted lines in Figure 7); however, in contrast to the case of **2**·1.5[$(CH_3)_2CO$], these interactions are intrastrand only and do not increase the dimensionality of the supramolecular structure.

Crystal Structure of 4·solv. The asymmetric unit contains four independent silver atoms, each with different environments, pictured in Figure 8, two independent *o*-$C_6H_4[CH_2OCH_2C(pz)_3]_2$ ligands, and three of the four expected triflate counterions. The obvious main difference in this structure is that the free pyrazolyl ring that was observed with **3** is coordinated to additional silver(I) cations. Both Ag(1) and Ag(2) are κ^2-coordinated by two pairs of tris(1-pyrazolyl)methane units from two separate ligands and have a distorted-tetrahedral arrangement of their nitrogen donor atoms, with the distortion imposed by the bite angle of the ligand, as with the first three compounds. Each tris(1-pyrazolyl)methane unit adopts the $\kappa^2-\kappa^1$ coordination mode with the third ring κ^1-coordinated to either Ag(3) or Ag(4). Ag(3) lies in a C_{2v} setting; its coordination sphere is filled with two nitrogen atoms from κ^1-pyrazolyl rings of two different tris(1-pyrazolyl)methane units and two oxygen atoms from two triflate anions. Ag(4) is in a three-coordinate, trigonal-planar environment with the sum of bond angles around the metal being 359.47°. As with Ag(3), it is bonded to two nitrogen atoms from the κ^1-pyrazolyl rings of two different tris(1-pyrazolyl)methane units but only one oxygen atom from a triflate anion. The fourth, unidentified triflate anion is located between the covalent network sheets (vide infra) and does not interact with Ag(4).

This coordination mode of the *o*-$C_6H_4[CH_2OCH_2C(pz)_3]_2$ ligand generates two directions of propagation of the covalent network in **4**·solv. One is along the *b* axis of the unit cell, pictured left in Figure 9, produced by the opposite orientation of the coordination vectors of the chelating, κ^2-pyrazolyl ring pairs of two [$C(pz)_3$] units linked by the central arene ring. The second direction is along the *a* axis, generated by the remaining κ^1-pyrazolyl rings coordinated to Ag3 and Ag4 atoms, pictured right in Figure 9.

The two independent $\mathbf{L^3}$ ligands have different orientations of the side arms. From left to right in Figure 9, the first ligand has one of its side arms (CH_2-O-CH_2 set of atoms) bent out of the plane with the central arene ring, while the other is lying in the plane. The second ligand has both side arms bent out of the plane and oriented in different directions with respect to the central arene ring plane.

The overall covalent network is a planar sheet, pictured in Figure 10. These sheets do not interact between themselves. They are separated by a large solvent area, representing 29.7% of the total unit cell volume.

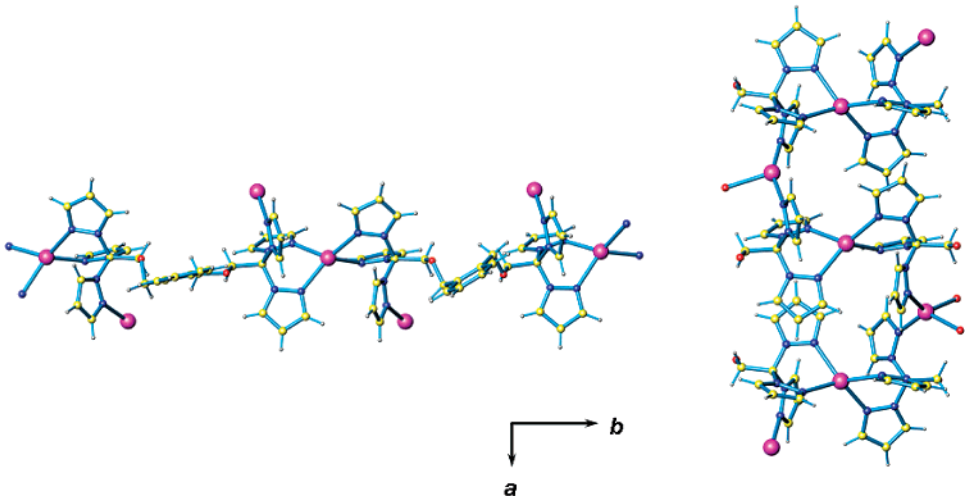

Figure 9. Coordination mode of $\mathbf{L}^3$ in **4**·solv: (left) the chelating behavior of the ligand along the *b* axis; (right) the bridging behavior along the *a* axis.

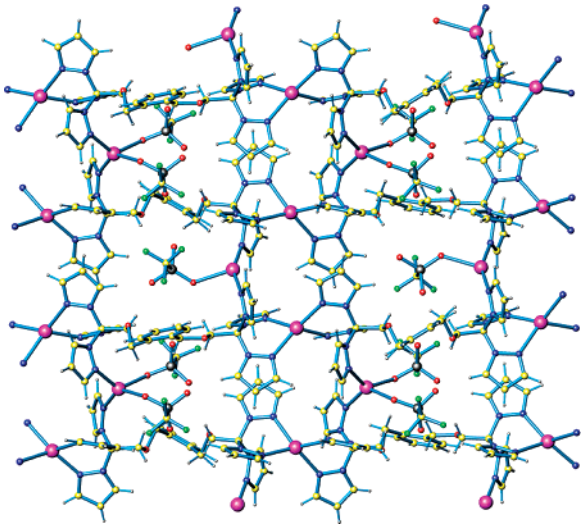

Figure 10. Overall 2D covalent framework in **4**·solv.

Discussion

The polymeric strands of **1**·2[$(CH_3)_2CO$] and **2**·1.5[$(CH_3)_2$-CO] are practically identical when one compares their covalent frameworks (compare Figure 2 with Figure 4), not only with respect to the silver environment but also in the overall arrangement of the ligands. Both compounds of the new ligand have their metallic centers in a tetrahedral environment, with minor differences in the bond lengths and angles (see Table 2).

The parameter τ_4 (eq 1), recently proposed by Houser et al.,[17] describes the geometry of a four-coordinate system and allows for a numerical comparison between different four-coordinate systems.

$$\tau_4 = \frac{360° - (\alpha + \beta)}{141°} \qquad (1)$$

where α and β are the largest angles in the four-coordinate species.

When τ_4 is zero, a square-planar geometry is described, and when τ_4 is 1.00, a tetrahedral geometry is described.[17]

(17) Yang, L.; Powell, D. R.; Houser, R. P. *Dalton Trans.* **2007**, 955.

Table 4. τ_4 Parameters for **1**·2[$(CH_3)_2CO$], **2**·1.5[$(CH_3)_2CO$], **3**, and **4**·solv

compound	silver	τ_4
1·2[$(CH_3)_2CO$]	Ag(1)	0.71
2·1.5[$(CH_3)_2CO$]	Ag(1)	0.73
3	Ag(1)	0.26
4·solv	Ag(1)	0.70
	Ag(2)	0.66
	Ag(3)	0.64

Table 4 gives the τ_4 parameters for all the four-coordinate silver atoms in **1**·2[$(CH_3)_2CO$], **2**·1.5[$(CH_3)_2CO$], **3**, and **4**·solv. The τ_4 numbers for **1**·2[$(CH_3)_2CO$] and **2**·1.5[$(CH_3)_2$-CO] are 0.71 and 0.73, respectively, which indicates that the two silver atoms in these compounds lie in a distorted-tetrahedral environment that is very similar. Also, in both compounds, the ligands have their side arms in the same orientation with respect to the central arene ring. Both strands are supported by similar pyrazolyl−central arene ring CH···π interactions, which are of approximately equal strength as based on their geometrical characteristics. The supramolecular structure of the strands is also similar: Two strands are interdigitated (Figure 3) and held together by the means of two CH···π interactions.

The differences in their supramolecular structure are a result of the different hydrogen-bonding capabilities of the counterions. While the PF_6^- anion is not such a good hydrogen acceptor, the $CF_3SO_3^-$ group is known to be largely implicated in both hydrogen bonds and anion−silver interactions. In the case of **2**·1.5[$(CH_3)_2CO$], where the silver(I) centers are coordinatively saturated by two bis(1-pyrazolyl)-methane groups, the triflate anion is involved only in strong hydrogen bonds, organizing the dimeric strands into a 2D sheetlike structure (see Figure 5). No such organization is present in **1**·2[$(CH_3)_2CO$].

An additional pyrazolyl ring in each sidearm of **3** yields an overall structure that is similar to that of **1** and **2.** Each tris(1-pyrazolyl)methane unit bonds two silver atoms in a $\kappa^2-\kappa^0$ fashion, forming a polymer chain with the central arene rings situated on the same side of the chains, as observed in all three compounds. The additional pyrazolyl ring impacts the coordination geometry about the silver

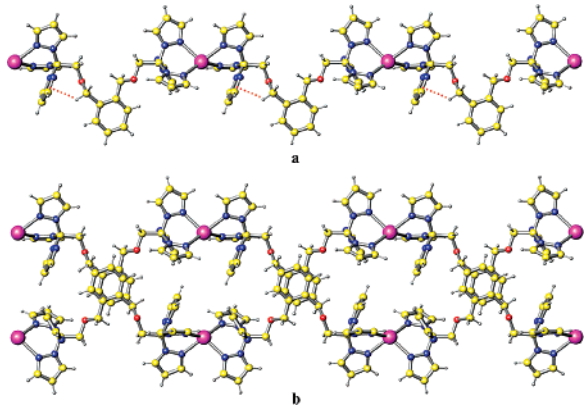

Figure 11. (a) One polymeric chain of **5**; note the CH···π interaction made by every second nonbonded pyrazolyl ring with a CH_2 group; (b) two strands of **5**, organized in polymeric dimers through a $\pi-\pi$ stacking interaction between the central arene rings.

atoms, which is between that of a tetrahedral and square-planar environment for **3**, indicated by τ_4 having a value of 0.26. We have previously demonstrated that increasing the size of the substituents on the central carbon of bis(1-pyrazolyl)methane ligands (e.g., κ^2-$Ph_2C(pz)_2$) favors square-planar geometry about silver(I).[11l]

The additional pyrazolyl unit brings important changes in the structural characteristics of the compounds; the noncovalent interactions supporting the chains are different. Half of the noncoordinated pyrazolyl rings interact along the covalent framework through CH···π interaction (see Figure 7) between these pyrazolyl rings and one hydrogen atom from the methylene groups next to the central arene ring, and the other half is involved in hydrogen bonds with oxygen atoms from the $CF_3SO_3^-$ ion. These triflate anions are situated along the chain, being involved in intrastrand hydrogen bonds, (Figure 7) and in contrast with **2**·1.5[$(CH_3)_2$-CO], do not increase the dimensionality of the supramolecular structure of **3**.

The triflate anions in **3** also cause an important structural change when this compound is compared with its BF_4^- analogue, $\{o\text{-}C_6H_4[CH_2OCH_2C(pz)_3]_2(AgBF_4)\}_n$ (**5**), previously published by us.[11h] The 1D covalent framework of **5** is similar with that of **3**, including the intrastrand CH···π interaction, showing the consistency of the $\mathbf{L^3}$ ligand (compare Figure 7 with Figure 11a). However, the strands in **5** are organized into dimers, shown in Figure 11b, through a face-to-face $\pi-\pi$ stacking between the central arene rings, and the BF_4^- anions further increase the dimensionality of these dimeric strands into a 3D noncovalent architecture. This additional organization is not observed with **3**, due to a different anion, with different structural and hydrogen-bonding characteristics.

The structure of **4**·solv demonstrates that in the presence of excess AgO_3SCF_3 the "free" pyrazolyl ring observed in **3** can be utilized to bond additional silver(I) centers. Interestingly, the coordination of this pyrazolyl ring seems to lower its steric influence on the geometries about the four-coordinate Ag(1) and Ag(2) atoms, which now are closer to the distorted-tetrahedral arrangement of **1** and **2** than the nearly square-planar arrangement observed with **3**. Again,

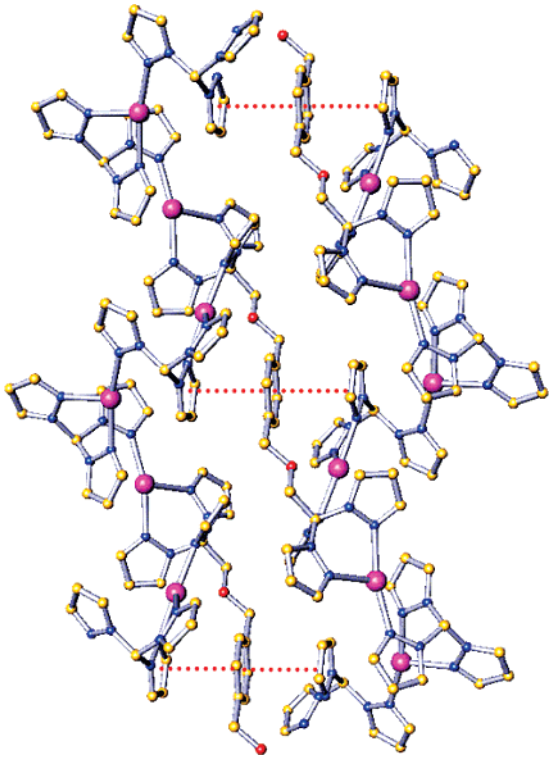

Figure 12. View of two adjacent helical argentachains for $\{p\text{-}C_6H_4[CH_2OCH_2C(pz)_3]_2(AgCF_3SO_3)_2\}_n$ (**6**), showing the $\kappa^2-\kappa^1$ coordination mode of the $[C(pz)_3]$ donor set.

this can be seen numerically using the τ_4 index. Ag(1) and Ag(2) of **4**·solv have values of 0.70 and 0.66, which indicate a geometry closer to tetrahedral, compared with the τ_4 value of 0.26 seen in **3**. The additional bonding interactions convert the 1D structure in **3** to a more complicated 2D structure in **4**·solv in which each tris(1-pyrazolyl)methane unit in the $o\text{-}C_6H_4[CH_2OCH_2C(pz)_3]_2$ ligands adopt a $\kappa^2-\kappa^1$ coordination mode. Although the majority of the silver(I) complexes of the *m*- and $p\text{-}C_6H_4[CH_2OCH_2C(pz)_3]_2$ ligands adopt a $\kappa^2-\kappa^1$ coordination mode, the type of $\kappa^2-\kappa^1$ coordination mode observed in **4**·solv was not encountered previously. The typical $\kappa^2-\kappa^1$ bridging mode is exemplified in Figure 12 by-$\{p\text{-}C_6H_4[CH_2OCH_2C(pz)_3]_2(AgO_3SCF_3)_2\}_n$ (**6**).[11i] In this case, two pyrazolyl ligands from one $[C(pz)_3]$ donor set are coordinated to one Ag atom and the third pyrazolyl ring is coordinated to a second Ag atom. A second $[C(pz)_3]$ donor set, from another $p\text{-}C_6H_4[CH_2OCH_2C(pz)_3]_2$ ligand, chelates the second Ag atom which is monocoordinated by the first $[C(pz)_3]$ unit (see Figure 12). In this way, the silver centers are all tricoordinated by three pyrazolyl rings from two different $[C(pz)_3]$ units. In contrast, $\mathbf{L^3}$ has a different $\kappa^2-\kappa^1$ behavior in **4**·solv: Two pyrazolyl ligands from one $[C(pz)_3]$ donor set are coordinated to one Ag atom, and the third pyrazolyl ring is coordinated to a second Ag atom that is not further chelated by a second $[C(pz)_3]$ donor set from another ligand but rather κ^1-coordinated by one pyrazolyl ring, as pictured in Figure 9.

Another interesting structural feature is the orientation of the side arms of the $\mathbf{L^2}$ and $\mathbf{L^3}$ ligands relative to the central arene ring. In our previous conformational analysis on free ligand $\mathbf{L^3}$ using the *Spartan 02* package,[11h] molecular orbital

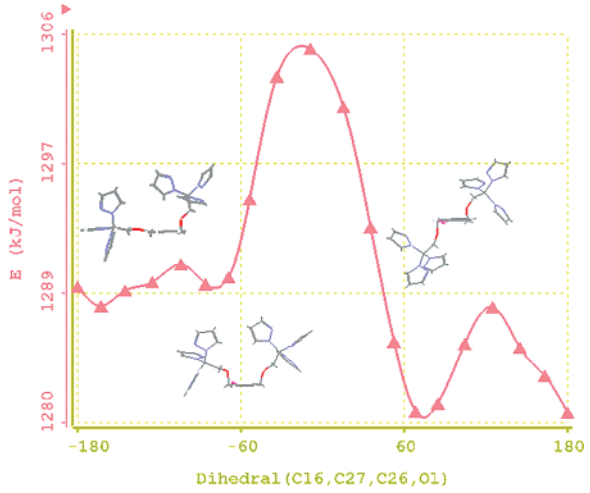

Figure 13. Three classes of conformers for $\mathbf{L^3}$; from left to right they are noted as in-plane_up, up_up, and up_down.

calculations at the PM3 semiempirical level revealed the existence of three classes of conformers (noted as "up_up", "up_down" and "in-plane_up" with respect to the orientation of the side arms). Figure 13 shows the variation of the enthalpy of formation (in gas phase) with the C16−C27−C26−O1 dihedral (defining the rotation of the pyrazolyl fragment around the arene−carbon bond). These data suggest that the most favored conformer is the up_down one, and it is separated by ca. 18−20 kJ/mol from the up_up and in-plane_up conformers. The lowest energy conformer in the gas phase differs from that observed in the solid-state structure of the free ligand $\mathbf{L^3}$.[11a,h] In this structure, the association between the $\mathbf{L^3}$ molecules into dimers via CH···π interactions prevents the formation of the up_down conformer and leads to the observed in-plane_up conformer. In contrast, in other cases with similar ligands where such CH···π interactions do not exist, the observed up_down orientation of the side arms in the solid-state structure matches that predicted by theory, as is the case for the 1,2,4,5-$C_6H_2[CH_2OCH_2C(pz)_3]_4$ ligand (for details, see ref 11h).

The solid-state supramolecular structures of **1**·2[$(CH_3)_2$CO] and **2**·1.5[$(CH_3)_2$CO] are based on CH···π interactions similar to those observed for $\mathbf{L^3}$ (Figure 3). As can be seen in Figures 2 and 4, the orientation of the side arms of the ligands of these complexes is in-plane_up in both cases, as observed for $\mathbf{L^3}$. In the case of **3**, where no such CH···π interactions are found, the orientation of the side arms of the ligand is that of the predicted up_down. This analysis cannot be extended to **4**·solv, where the ligand adopts both the in-plane_up and up_down conformers, because these arrangements are due to the covalent forces that built up the 2D framework.

Conclusion

This paper reports our first successful attempt to increase our third-generation family of tris(1-pyrazolyl)methane-based ligands with the general formula $C_6H_{6-n}[CH_2OCH_2C(pz)_3]_n$ (n = 2, 3, 4, 6) to a more general class, with a general formula $C_6H_{6-n}[CH_2OCH_2CH_{3-x}(pz)_x]_n$ (n = 2, 3, 4, 6; x = 2, 3).

The major structural characteristic of all the complexes with silver(I) as the metal and ligands with the tris(1-pyrazolyl)methane donor set linked by a central arene ring in the ortho position is that these ligands strongly favor the $\kappa^2-\kappa^0$ bonding mode. The covalent framework is 1D, but the crystal packing is influenced by a combination of noncovalent interactions. The counter ions also impose changes in the overall structures of the crystalline solids. When the new ligand based on bis(1-pyrazolyl)methane units was used, a similar 1D covalent network was obtained, and supramolecular similarities were also found in their crystal packing.

These results show again that the two opposed structural characteristics built into the $C_6H_{6-n}[CH_2OCH_2CH_{3-x}(pz)_x]_n$ family of ligands (rigid groups and flexible linkers) are complementary; while the rigid groups definitely support special organizational features within the structures, the flexible linkers allow all these features to manifest themselves in a cumulative and complementary manner. We have also shown that several important structural characteristics are common to the bis- and tris(1-pyrazolyl)methane-based ligands, demonstrating that organizational features can be transferred from one case to another. Finally, we have shown with **4**·solv that it is possible to use the free pyrazolyl ring in cases where tris(1-pyrazolyl)methane units are in the $\kappa^2-\kappa^0$ bonding mode to expand the covalent framework from 1D to 2D.

Acknowledgment. We thank the National Science Foundation (CHE-0715559) for financial support. We also thank Dr. Russell Watson for his advice on ligand synthesis.

Supporting Information Available: CIF file. This material is available free of charge via the Internet at http://pubs.acs.org.

IC7017743